

Keywords: vibrations; vibratory conveyor; dynamic eliminator; transport stop; feeder; reverse transport

Weronika ŻMUDA^{1*}, Piotr CZUBAK²

INVESTIGATIONS OF THE TRANSPORT POSSIBILITIES OF A NEW VIBRATORY CONVEYOR EQUIPPED WITH A SINGLE ELECTRO-VIBRATOR

Summary. In the present study, a new vibratory conveyor (patent pending) equipped with a single electro-vibrator intended for an accurate material dosage is investigated. The possibilities of material transportation in the circum-resonant zone were investigated analytically and by simulations [1]. Furthermore, the dependencies of the transport velocity of the tested conveyor as functions of the excitation frequency were determined. Favorable excitation frequencies at transports in the main and reversal directions were found, and the high usefulness of the machine in the production lines requiring accurate material dosage was indicated. A control strategy allowing for a sudden stop of the transported material was also proposed.

1. INTRODUCTION

Vibratory conveyor systems are widely used in various industries. This is because of their working characteristics and the possibility of transporting granular materials of different sizes and with different physical and chemical characteristics [2]. In the significant number of different production lines, there is often a need to stop a feed transport or to dosage it [3, 4, 5]. Classic structures [6] driven by a system of electro-vibrators are not usually suitable for intermittent running since their electro-vibrators must be switched off in order to stop the feed transport. This causes the machine to pass through the resonance zones, due to which the vibration amplitude usually increases, making it impossible to control transport velocity. A conveyor with the possibility of sieving is an example of such a structure [7].

There are also solutions with kinematic excitation [1] that ensure total control over device operations. However, these are characterized by several negative aspects, such as an abrasion in joining points and the occurrence of clearances.

Devices driven by electromagnetic excitations and characterized by a high control accuracy of a transport velocity are also known [8]. These types of structures are generally applied for dosing the material being transported. However, such devices have higher purchase costs due to the type of drive used. Their dimensions and inertia, which are very often large, are additional limitations of such solutions [4]. Additionally, conveyors equipped with an electromagnetic drive are much less durable than other conveyors.

Very often, solutions of vibratory conveyors are characterized by the use of more than one inertial drive. Examples of such conveyors, in which a system of two electro-vibrators allowing the accurate dosing of materials is applied, are patented devices, the dynamic properties of which have been analyzed in the scientific literature [3].

¹ AGH University of Science and Technology, Doctoral School; 30 Mickiewicza Alley, Building D-1, Kraków 30-059, Poland; e-mail: wezmuda@agh.edu.pl; orcid.org/0000-0002-8632-9266

² AGH University of Science and Technology, Faculty of Mechanical Engineering and Robotics; 30 Mickiewicza Alley, Building D-1, Kraków 30-059, Poland; e-mail: czubak@agh.edu.pl; orcid.org/0000-0001-8030-7173

* Corresponding author. E-mail: wezmuda@agh.edu.pl

The solution of the dosing conveyor equipped with a single electro-vibrator, which allows the transport process to be stopped suddenly [3] and an inverse transport of a slow velocity to be obtained is proposed in the present paper. One of the advantages of this new solution is a lack of problems related to the self-synchronization of electro-vibrators [9] and the energy-saving system due to the use of a single motor. Therefore, the device is highly desirable across industries [10] and, hence, has a very high potential for industrial use.

2. SCHEME OF THE CONVEYOR AND PRINCIPLE OF ITS OPERATIONS

A schematic representation of the proposed solution is presented in Fig. 1.

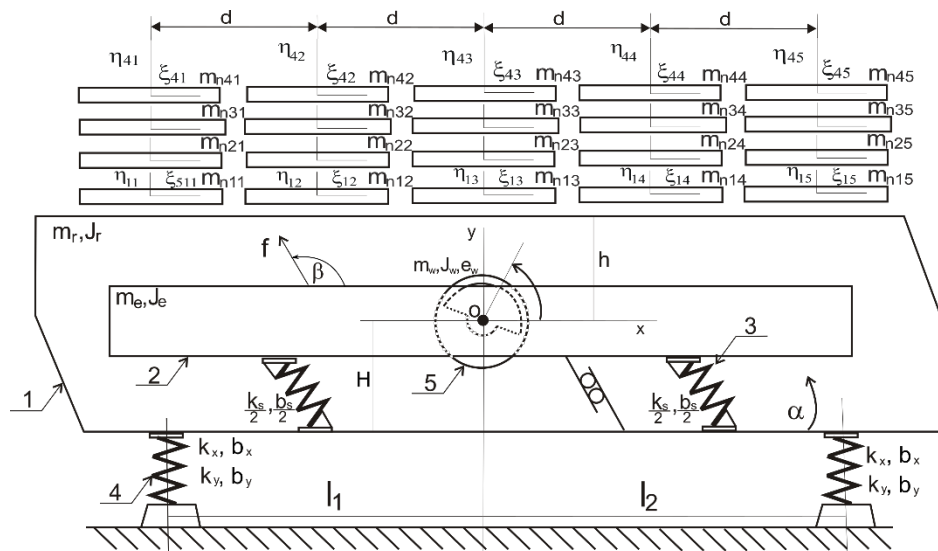


Fig. 1. Schematic representation of the solution, along with the feed model

The conveyor (patent pending no. P. 441218) is equipped with one electro-vibrator (5) suspended to the trough (1). The mass of the eliminator (2) on the suspension consisting of a system of leaf springs (3) is added to the mass of the body (1). The aim of the smaller mass (2) is to eliminate trough vibrations in the f direction. In a specially adapted way of controlling the excitation frequency of electro-vibrators, according to the Frahm's eliminator rule [11, 12, 13, 14, 15], the trough vibrations in the f direction fade away, while vibrations in the perpendicular direction are not changed.

When the single vibrator is applied, the device suspended on the classic suspension will perform movements similar to the circle in Fig. 5b. In the situation presented in Fig. 5b, for clockwise rotations, the material is transported at a low velocity to the left. When the vibration frequency of the electro-vibrator constitutes the vibration frequency of the mass of the eliminator on the system of leaf springs, this mass acts as Frahm's eliminator, removing (in practice) vibrations of the system in the direction of the eliminator vibrations without influencing the vibrations in the perpendicular one [16].

$$\omega_{el} = \sqrt{k_{el}/m_{el}} \quad (1)$$

Vibrations' effects are eliminated independently of the natural vibrations frequency of the initial system before eliminator connection. The Frahm's eliminator system operates in the antiresonance valley [17], which is surrounded by resonance zones. Moreover, the size of this valley depends on the proportion of the smaller mass (mass of eliminator) to the mass of the body [18, 19]. At such a frequency, the trough performs vibrations (shown in approximation in Fig. 5a), allowing the feed to transport to the right.

According to the operating strategy of the device, there is no need to switch the engine off to stop the transportation; thus, the system has no need to pass the resonance zones. When the excitation frequency of vibrations (the rotations of a vibrator) is decreased in such a way that the additional mass

will not operate as the Frahm's dynamic eliminator, the feed flow will stop. As the rotary frequency of the unbalanced mass decreases further, the material is slowly transported in the opposite direction (i.e., to the left).

The transport stoppage can be achieved in a relatively short time, just needed for changing the electro-vibrator rotation frequency causing trough vibrations of a circular character (Fig. 5b). The transport restarts when the excitation frequency of the unbalanced mass returns to a partial frequency of the additional mass on its own suspension ω_{el} . At that time, the character of vibrations will be again similar to the one presented in Fig. 5a and will cause a fast restart of the transport to the right. The transport is of a velocity typical for this class of machines.

The model of the system consists of a dynamical equation describing the behavior of the machine (4), which was derived from the Lagrange function (2) of the system and dissipation model (3), equations of the motor drive (13), equations describing the movement of the transported material layers (11, 12), and equations describing normal (9) and tangent (10), and the influences between feed layers and between the first layer and the trough [7]. Because the model is a five DOF system with four additional consecutive layers of the feed divided into five separate columns, the mathematical model consists of five equations of motion of the conveyor, together with the two equations of motion of one particle of the feed. Thus, 40 equations concerning the feed are presented in the shortened scheme consisting of indexes j, k .

$$L = E - U = \frac{1}{2}[m_r(\dot{x}^2 + \dot{y}^2) + m_e((\dot{x} + \dot{f} \cos \beta)^2 + (\dot{y} + \dot{f} \sin \beta)^2) + m_w((\dot{x} - e\dot{\varphi} \sin \varphi)^2 + (\dot{y} + e\dot{\varphi} \cos \varphi)^2) + J_r\dot{\alpha}^2 + J_e\dot{\alpha}^2 + J_w\dot{\varphi}^2] - \quad (2)$$

$$-k_x(x + H\alpha)^2 - \frac{1}{2}k_y(y + l_1\alpha)^2 - \frac{1}{2}k_y(y - l_2\alpha)^2 - \frac{1}{2}k_s f^2$$

$$N = 2b_x(\dot{x} + H\dot{\alpha})^2 + b_y(\dot{y} + l_1\dot{\alpha})^2 + b_y(\dot{y} - l_2\dot{\alpha})^2 + b_s\dot{f}^2 \quad (3)$$

$$M \cdot \ddot{q} = Q \quad (4)$$

$$M = \begin{bmatrix} m_r + m_w + m_e & 0 & 0 & m_w \sin(\varphi) & m_e \cos(\beta) \\ 0 & m_r + m_w + m_e & 0 & m_w \cos(\varphi) & m_e \sin(\beta) \\ 0 & 0 & J_r + J_e & 0 & 0 \\ m_w \sin(\varphi) & m_w \cos(\varphi) & 0 & m_w e^2 + J_w & 0 \\ m_e \cos(\beta) & m_e \sin(\beta) & 0 & 0 & m_e \end{bmatrix} \quad (5)$$

$$\ddot{q} = [\ddot{x} \quad \ddot{y} \quad \ddot{\alpha} \quad \ddot{\varphi} \quad \ddot{f}]^T \quad (6)$$

$$Q = \begin{bmatrix} -m_w e \varphi^2 \cos \varphi - 2k_x(x + H\alpha) - 2b_x(\dot{x} + H\dot{\alpha}) - T_{101} - T_{102} - T_{103} - T_{104} - T_{105} \\ m_w e \varphi^2 \sin \varphi - k_y(y + l_1\alpha) - k_y(y - l_2\alpha) - b_y(\dot{y} + l_1\dot{\alpha}) - b_y(\dot{y} - l_2\dot{\alpha}) - F_{101} - F_{102} - F_{103} - F_{104} - F_{105} \\ -2k_x H^2 \alpha - 2k_x H \dot{x} - 2b_x H \dot{\alpha} - 2b_x H^2 \ddot{\alpha} - k_y(y + l_1\alpha)l_1 + k_y(y - l_2\alpha)l_2 - b_y(\dot{y} + l_1\dot{\alpha})l_1 + b_y(\dot{y} - l_2\dot{\alpha})l_2 + \\ (T_{101} + T_{102} + T_{103} + T_{104} + T_{105})h + F_{101}2d + F_{102}d - F_{104}d - F_{105}2d \\ M_{el} - b_f \dot{\varphi} \sin \varphi \\ -k_s f - b_s \dot{f} \end{bmatrix} \quad (7)$$

where:

$F_{j,j-1,k}$ – perpendicular element of j layer pressure on $j-1$ in k column,

$T_{j,j-1,k}$ – horizontal element of j layer pressure on $j-1$ in k column,

j – index of the feed layer, $j=0$ relates to the machine body,

k – index of the column of the feed layer.

If there is no contact between consecutive layers of the feed, then

$$F_{j,j-1,k} = 0, T_{j,j-1,k} = 0 \text{ for } \eta_{j,k} \geq \eta_{j-1,k} \quad (8)$$

However, if contact occurs, according to the model [20, 21], the equations take the form of

$$F_{j,j-1,k} = (\eta_{j-1,k} - \eta_{j,k})^p \cdot k \cdot \left\{ 1 - \frac{1-R^2}{2} \left[1 - \text{sgn}(\eta_{j-1,k} - \eta_{j,k}) \cdot \text{sgn}(\dot{\eta}_{j-1,k} - \dot{\eta}_{j,k}) \right] \right\}, \quad (9)$$

$$T_{j,j-1,k} = -\mu F_{j,j-1,k} \text{sgn} \left(\dot{\xi}_{j,k} - \dot{\xi}_{j-1,k} \right), \quad (10)$$

where:

k and p – Herz-Sztajerman constants,

R – coefficient of restitution.

Feed layers equations in directions ξ and η have the following form:

$$m_{nj,k} \ddot{\xi} = T_{jj-1,k} - T_{j+1,j,k} \quad , \quad (11)$$

$$m_{nj,k} \ddot{\eta} = -m_{nj,k} g + F_{jj-1,k} - F_{j+1,j,k} \quad , \quad (12)$$

M_{eli} – electromagnetic moment is developed from the Kloss equation:

$$M_{eli} = \frac{2M_{ut}(\omega_{ss} - \dot{\varphi}_i)(\omega_{ss} - \omega_{ut})}{(\omega_{ss} - \omega_{ut})^2 + (\omega_{ss} - \dot{\varphi}_i)^2} \quad , \quad i=1 \quad , \quad (13)$$

where:

M_{ut} – stalling torque,

ω_{ss} – synchronous frequency,

ω_{ut} – frequency of stall.

Table 1

Values of parameters simulations were performed for

Parameter	Value	Unit	Description
$l_1 = l_2$	0.365	[m]	Distance between the center of rotation to the axis of a spring
$b_x = b_y$	33.2	[Ns/m]	Damping coefficient of the coil spring
$k_x = k_y$	32,000	[N/m]	Stiffness coefficient of the coil spring
b_s	52.8	[Ns/m]	Damping coefficient of the system of leaf springs
k_s	1,041,519	[N/m]	Stiffness coefficient of the system of leaf springs
m_e	42.5	[kg]	Eliminator mass
m_r	65	[Kg]	Body mass
m_w	6	[Kg]	Unbalanced mass
m_n	4	[Kg]	Mass of the feed
J_e	3.7	[kgm ²]	Eliminator's moment of inertia
J_r	4.82	[kgm ²]	Main mass's moment of inertia
J_w	0	[kgm ²]	Moment of inertia of the unbalanced mass
β	135	°	Working angle of the leaf springs
R	0.05	unitless	coefficient of restitution
μ	0.4	unitless	Friction ratio
p	1	unitless	Herz-Sztajerman constant
k	10 ⁸	[N/m]	Herz-Sztajerman constant
e	0.026	[m]	Unbalance position
H	0	[m]	Height between the center of mass and the spring position
m_{ut}	4.26	[Nm]	Maximum torque

3. SIMULATION INVESTIGATIONS

Simulations were performed via Pascal environment alongside Matlab as a tool for the treatment of the results. The equations presented in the previous section were implemented in the form of matrices together with the values presented in Table 1. Runge-Kutta of second- and third-order methods were used to solve introduced differential equations. Because during the operation of the system, there are many collisions of feed particles with each other, as well as of feed with the trough, the contact forces during the collision increase rapidly. Therefore, the use of the variable integration step causes its uncontrolled selection, which, in turn, leads to problems with computing power. In the case of these

simulations, the fixed-step method with a step of 10^{-5} was used, so the step is not uncontrollably customized.

Investigations of the transport velocity in the function of excitation frequency were performed for two directions of rotations [6, 20, 22]. Diagrams were generated for very small changes in the rotational frequency of electro-vibrators, achieving quasi-steady states.

The course of the average transport velocity for the electro-vibrator rotations to be in accordance with the clockwise rotations is presented in Fig. 2 (black curve). At such a direction of rotation, two directions of transportation, which allow the feed to move away from the trough edge (assuming accurate dosing), can be achieved.

During switching on and operations up to approximately 55 rad/s, material transportation does not occur. By increasing the angular frequency of the electro-vibrator, the material transportation to the left is achieved. Initially, the feed velocity gradually increases until the maximum velocity is obtained. Then, together with an increase in the excitation frequency, it falls to the work point, at which the transportation decays (at $\omega_{ss} = 135$ rad/s). This occurrence is caused by the fact that the material in the lower part of the ellipse is pressed more strongly against the trough than the material in the upper part since the centrifugal force of the material particle in the lower part adds to the gravity force while in the upper part subtracts from it. When the trough rotates clockwise, the particle in the lower part of the ellipse (when it is pressed to the trough) moves to the left, and therefore, we obtain transport to the left at frequencies between 55 and 135 rad/s.

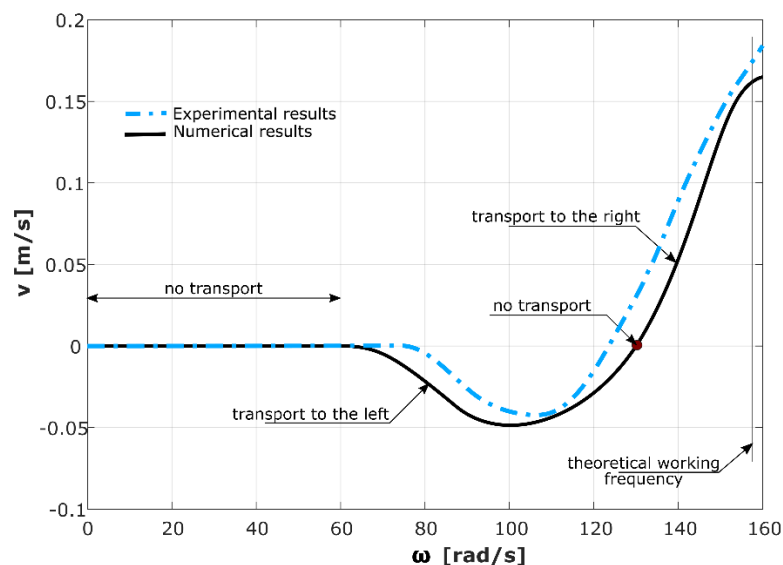


Fig. 2. Average transportation velocity of the feed vs. angular velocity of the drive (clockwise)

As the frequency of the electro-vibrator increases further, transportation occurs in the opposite direction. The maximum velocity occurs at a frequency higher than the antiresonance frequency, which should not be exceeded for constructional reasons (an excessive amplitude of the eliminator mass). It can be seen in the diagram that the transportation velocity is nearly a linear function of the rotary frequency of unbalanced mass, from the transport stoppage to its maximum velocity, which allows for the easy control of the transport velocity.

The analogous analysis was performed for the rotation of unbalanced mass in the opposite direction and is presented in Fig. 3 (black curve). The course of an average transport velocity, as the function of the rotary frequency of an unbalanced mass for quasi-steady states, was obtained. In a similar way, as can be seen in the simulation results shown in Fig. 2, the rated velocity was obtained at the work point of 157 rad/s. At such a direction of the electro-vibrator rotations, the transport either moves to the right or decays at a frequency below 55 rad/s. For this velocity course, it is not possible to move the feed aside from the trough edge; however, due to the relatively slow increase in the transport velocity depending on the angular velocity, a more precise dosing of the material can be achieved. As seen in

Fig. 3 (analogous to Fig. 2), the transport course is nearly a linear function, which, in these cases, also facilitates the transportation velocity control.

Successive simulations were performed for the exact cases of changes in the electro-vibrator rotation velocity. Fig. 4 presents three diagrams: the angular velocity of unbalanced mass (top) for the case of the clockwise rotation, transport velocity in time (middle), and the displacement of material (bottom).

The figure shows the course of the average transport speed as the time function (middle plot) and the feed displacement on the trough (bottom plot) depending on the angular velocity change (top). This analysis allows us to present clearly the possibilities of the material stoppage by changing the angular velocity of the electro-vibrator without switching it off and without the system passing via the resonance zones. Violent changes in the transport velocity of an average value of 0 are seen at starting of the device. After five seconds, slow material transport to the left occurs and then, up to the moment when the rated speed of 157 rad/s is obtained, the violent increase in the average transport velocity to its maximum value occurs. Through successive decreases of the excitation velocity to 135 rad/s, the transport stoppage is obtained. When the conveyor is switched off between 80 and 90 s, reverse transport is achieved. This results from the fact that, when coasting and decreasing the rotational velocity of the electro-vibrator, the transport (according to Fig. 2) will be to the left, which provides a certainty that the dosed material will not be poured from the trough during coasting.

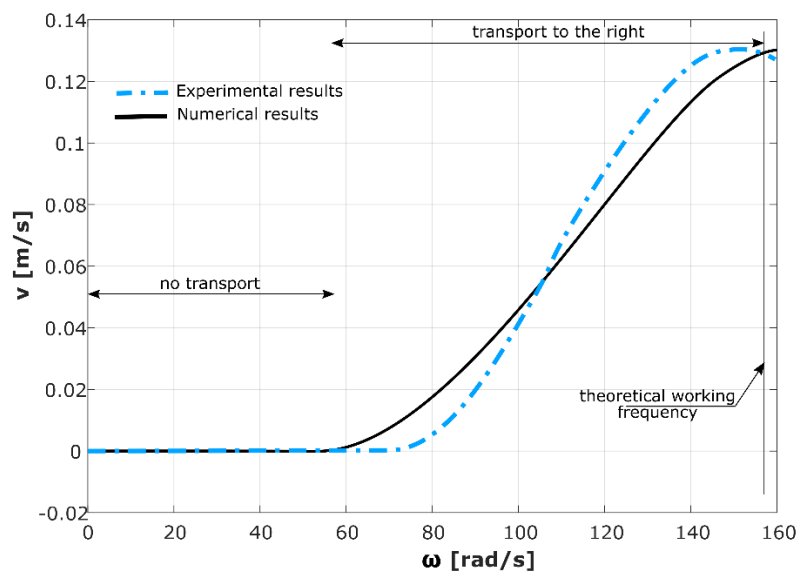


Fig. 3. Average transportation velocity of the feed vs. angular velocity of the drive (counterclockwise)

An analysis of the eliminator deflection is not presented on the graph, but the eliminator obtains the highest amplitudes at the maximal angular velocities, indicating a designed work point of 157 rad/s. However, these amplitudes are not above 3.5 mm and, therefore, are acceptable due to the material fatigue of the leaf springs. It should be remembered that the suspension is a relatively stiff leaf suspension or leaf spring suspension that is fatigue susceptible. This leaf spring suspension is necessary since the eliminator must be suspended directionally in order to eliminate vibrations of the main mass at the work point of $\omega=157$ rad/s in the direction inclined at an angle of 135 degrees (as can be seen in the scheme shown in Fig. 1), not influencing vibrations of the main mass in the perpendicular direction, thus making feed transport possible. The eliminator amplitude can be decreased by increasing its mass; however, this simultaneously causes an increase in the suspension stiffness.

Movements of the trough for individual frequencies of electro-vibrator rotations are shown in Figs. 5a and 5b. Fig. 5a presents trough displacements for the excitation frequency of 157 rad/s for the moment at which the eliminator moving in the work direction of leaf springs eliminates trough vibrations in this direction. Thus, only vibrations in the perpendicular direction along leaf springs are

obtained, and the material is transported at the highest velocity. Trough vibrations are shaped in such a way regardless of the direction of unbalanced mass.

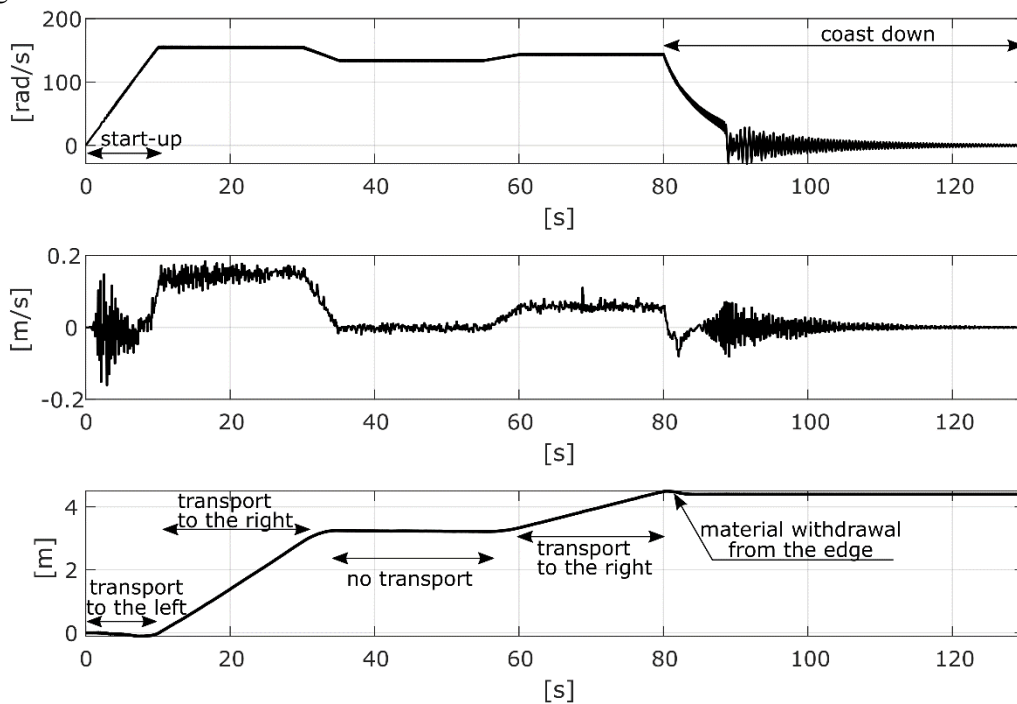
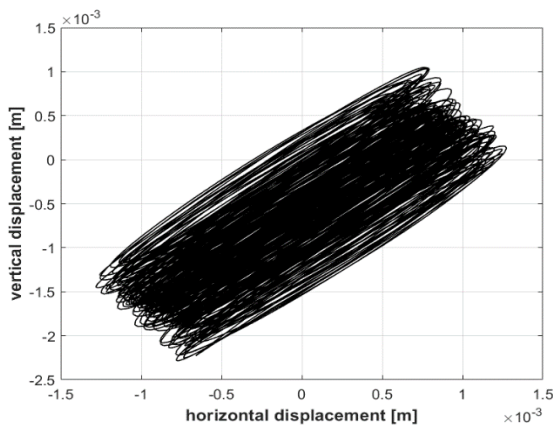


Fig. 4. Average velocity vs. time (top); displacement of the feed vs. time (middle); angular velocity vs. time (bottom) – clockwise

a)



b)

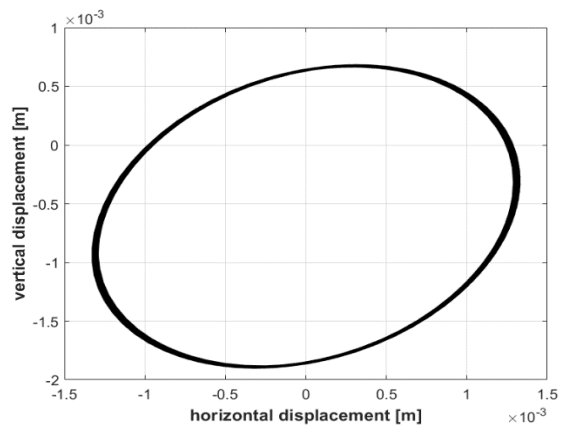


Fig. 5. a) Trough displacement at 157 rad/s; b) trough motion at 100 rad/s

Fig. 5b presents the trough motions for the rotation frequency of 100 rad/s. The diagram shows movements similar to a circle. When the excitation frequency equals 100 rad/s, the material is transported to the left at a low velocity (for the clockwise rotation of the unbalanced mass).

The simulations of the device operations for the unbalanced mass rotations in the opposite direction (i.e., for counterclockwise rotations) were performed in an analogous way.

Fig. 6 presents the angular velocity of unbalanced mass in time (top plot) for the case of the counterclockwise rotation, transport velocity vs. time (middle plot), and displacement of the material on the trough vs. time (bottom plot). When the electro-vibrator operates counterclockwise, material transport occurs in one direction only. During operations within the rated speed range, the transport to the right achieves the highest average velocity being 0.13 m/s. For the counterclockwise rotations of

unbalanced mass, there is a possibility of material dosage. As shown in Fig. 6, when the excitation frequency is decreased from 157 rad/s to 100 rad/s, the feed displacement on the trough is slower and equals approximately 0.07 m/s. Decreasing the frequency further would cause even slower transport, allowing for accurate dosage. The transport decays when rotations are smaller than 50 rad/s. Similarly, for the clockwise rotations, maximal amplitudes of the eliminator do not exceed 3.5 mm.

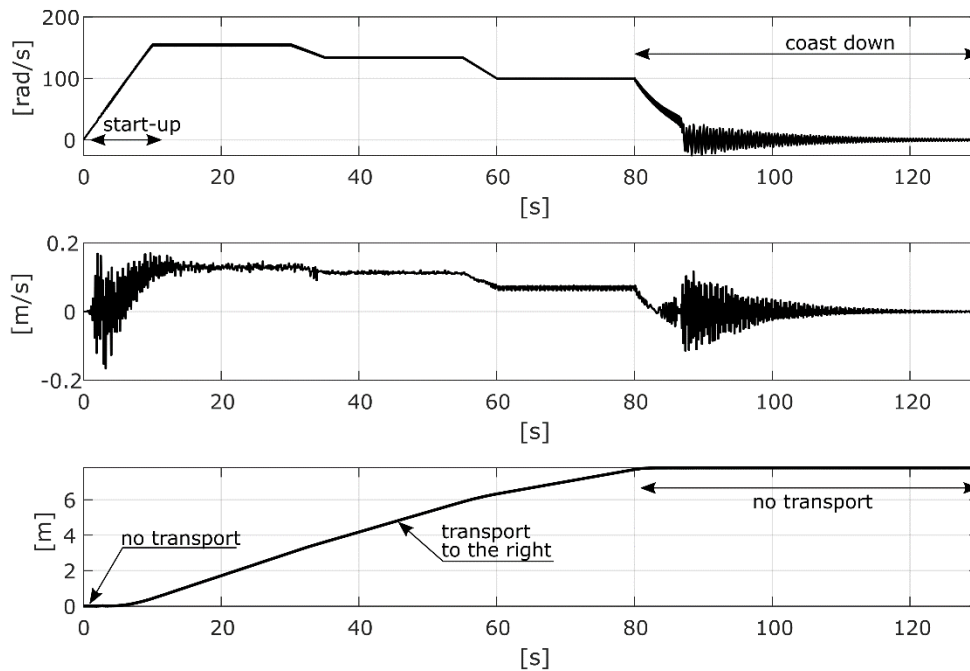


Fig. 6. Average velocity vs. time (top plot); displacement of the feed vs. time (middle plot); angular velocity vs. time (bottom plot) - counterclockwise

Based on the parameters determined in the present study, the project of the conveyor was designed (Fig. 7). The individual elements are numbered according to the scheme in Fig. 1.

Verification tests were performed on the conveyor. According to the results presented in Fig. 2 and Fig. 3 (indicated by the blue dotted curve), initial device performance predictions were confirmed. For the clockwise rotation of the unbalanced mass (Fig. 2), the average transportation velocity graph differs slightly from the simulated one with the width of the reverse transportation valley and with the start of transportation.

For the counterclockwise rotation of the unbalanced mass (Fig. 3), it is seen that the slope of the velocity function is slightly steeper than the predicted slope, which indicates a faster increase in the transportation velocity. While getting closer to the theoretical working frequency point, the velocity decreases slightly. The results of this research fully confirmed the idea and the principle of machine operation for both directions of rotation of the unbalanced mass. The differences in transportation velocity and the frequency at which transport stops are due to the specificity of the transported material. The test of the machine was carried out for sand, for which humidity varies depending on the environment.

3. CONCLUSIONS

Several conclusions can be drawn from the simulation studies performed in this work.

1. The conveyor indicates good transporting properties allowing it to be installed in production lines requiring feed dosage.

2. Dosage is performed by changes in the excitation frequency without the need to pass through resonance zones.
3. The conveyor doses a material regardless of the direction of the electro-vibrator rotations.
4. The work characteristics of the conveyor when the electro-vibrator rotates clockwise seem more advantageous because they allow the possibility of the spontaneous moving aside of feed from the conveyor edge during coasting. There is also a possibility of reversing the running direction.
5. Maximal amplitudes of eliminators are admissible on account of the material's strength.
6. The investigation of the speed of transport on the device fully confirmed the working principle of the new dosing conveyor, and their results were largely consistent with the results of the simulation tests.



Fig. 7. Machine according to the design

Acknowledgments

The work is included in the framework of the Department of Mechanics and Vibroacoustics.
16.16.130.942

References

1. US 5979640 *Vibrating conveyor drive with continuously adjustable stroke*. Publ. 091.11.1997.
2. Kipriyanov, F. & Savinykh, P. The results of the study of the vibratory conveying machine operating modes. *Transportation Research Procedia*. 2022. Vol. 63. P. 721-729.
3. Czubak, P. & Surówka, W. Influence of the Excitation Frequency on Operations of the Vibratory Conveyor Allowing for a Sudden Stopping of the Transport. *Vibrations in Physical Systems*. 2020. Vol. 31. No. 3. P. 1-12.
4. Surówka, W. & Czubak, P. Numerical review of selected solutions of vibratory feeders capable of dosing feed material. *Vibrations in Physical Systems*. 2020. Vol. 31. No. 3. P. 1-8.
5. Zejer, T. & Olesiński, M. & Musioł, K. & Okoń, T. Stopping Material Transport on Vibrating Feeder Chute, In: *International Colloquium Dymamesi 2021 – Dynamics of Machines and Mechanical Systems with Interactions*. Cracow (Poland). March 2-3, 2021.

6. Winkler, G. Analysing the vibrating conveyor. *International Journal of Mechanics*. 1978. Vol. 20. No. 9. P. 561-570.
7. US 4771894. *Device for separating materials of value from a mixture*. Publ. 20.09.1988.
8. US 6253908 B1. *Vibratory conveyor*. Publ. 03.07.2001.
9. Blekhman, I.I. & Izrailevich, I. *Synchronization in science and technology*. ASME press, 1988.
10. Polishchuk, L. & Khmara, O. & Piontkevych, O. & Adler, O. & Tungatarova, A. & Kozbakova, A. Dynamics of the conveyor speed stabilization system at variable loads. *Informatyka, Automatyka, Pomiarzy W Gospodarce i Ochronie Środowiska*. 2022. Vol. 12. No. 2. P. 60-63.
11. Despotović, Ž.V. & Urukalo, D. & Lečić, M.R. & Ćosić, A. Mathematical modeling of resonant linear vibratory conveyor with electromagnetic excitation: simulations and experimental results. *Applied Mathematical Modelling*. 2017. Vol. 41. P. 1-24.
12. US 989958 A. *Device for Damping Vibrations of Bodies*. Publ. 18.04.1911.
13. Gupta, Y.P. & Chandrasekaran, A.R. Absorber System for Earthquake Excitations. In: *Proceeding of the Fourth World Conference on Earthquake Engineering*. Santiago, Chile. January 1969. P. 139-148.
14. Hou, Y. & Peng, H. & Fang, P. & Zou, M. & Liang, L. & Che, H. Synchronous characteristics of two excited motors in an anti-resonance system. *Journal of Advanced Mechanical Design, Systems, and Manufacturin*. 2019. Vol. 13. No. 3. P. 1-14.
15. US 2951581 A. *Vibratory Conveyors*. Publ. 06.09.1960.
16. Khalil Gazi Md. & Shahidul Islam Md. An analytical study of vibration neutralizers. *Indian Journal of Engineering & Material Science*. 1999. Vol. 6. P. 256-262.
17. Richiede, D. & Tamellini, I. & Trevisani, A. *A general approach for antiresonance assignment in undamped vibrating systems exploiting auxiliary systems*. In: Uhl T. (eds). *Advances in Mechanism and Machine Science*. 2019. Vol. 73. P. 4085-4094.
18. Despotović, Ž.V. & Lečić, M.R. & Djuric, A. Vibration control of resonant vibratory feeders with electromagnetic excitation. *FME Transactions*. 2014. Vol. 42. No. 4. P. 281-289.
19. Liu, J. & LI, Y. & LIU, J. & Xu, H. Dynamical analysis and control of driving point anti-resonant vibrating machine based on amplitude stability. *Chinese Journal of Mechanical Engineering*. 2006. Vol. 1. P. 145-148.
20. Michalczyk, J. Phenomenon of Force Impulse Restitution in Collision Modelling. *Journal of Theoretical and Applied Mechanics*. 2008. Vol. 46. No. 4. P. 897-908.
21. Michalczyk, J. & Gajowy, M. Operational properties of vibratory conveyors of the antiresonance type. *Archives of Mining Sciences*. 2018. Vol. 63. No. 2. P. 301-319.
22. Lim, G.H. On the conveying velocity of a vibratory feeder. *Computers & Structures*. 1997. Vol. 62. No. 1. P. 197-203.

Received 13.08.2021; accepted in revised form 29.11.2022